VERSITA

Acta Geophysica
vol. 61, no. 6, Dec. 2013, pp. 1598-1625
DOI: 10.2478/s11600-013-0150-0

Field Experiment in Soultz-sous-Forêts, 1993: Changes of the Pattern of Induced Seismicity

Vladimir SMIRNOV[1,2], Alexander PONOMAREV[1], Pascal BERNARD[3], and Seid BOUROUIS[3]

[1]Schmidt Institute of the Physics of the Earth, Russian Academy of Sciences, Moscow, Russia; e-mail: avp@ifz.ru

[2]Lomonosov Moscow State University, Faculty of Physics, Moscow, Russia; e-mails: vs60@phys.msu.ru, vs60@mail.ru (corresponding author)

[3]Institut de Physique du Globe de Paris, Paris, France
e-mails: bernard@ipgp.fr, bourouis@ipgp.fr

Abstract

The data of the known field experiment on water injection in the borehole were analyzed. Parameters of self-similarity of seismicity were estimated in comparison with the changes of water pressure. Changes of seismicity parameters that indicate the redistribution of the failure from lower scales to upper are revealed. The total number of earthquakes per series of the water initiation found to be depended exponentially on the water pressure and seismic activity maximum is delayed gradually relative to beginning of initiation. The growth of induced seismicity zone in time differs from diffusion model for water flow in the porous medium. Analysis carried out from laboratory data indicates that diffusion growth of the failure area may be realized in the dry specimen, without fluid. It could be assumed that both kinetic processes – water and the failure diffusion – can be significant for the development of seismicity induced by the water injection.

Key words: induced seismicity, seismicity parameters, diffusion, kinetic process.

1. INTRODUCTION

Field modeling is powerful tools for investigation of the nature of seismicity. Man-made initiation allows to analyze origination and evolution of seismicity under natural condition, that makes possible to fill the gap between laboratory experiments and field investigation of seismicity.

An investigations of the background seismicity is complicated by the absence of information about the cause and source of seismicity variations. The seismic process involves different-type feedbacks that determine and control the evolution of seismicity. It is difficult to reveal and study these feedbacks in stationary conditions, since the variations in the background seismicity are insignificant, and their nature is usually poorly known. The transient mode of the seismic process is a response of the geophysical medium to the different impacts that disturb its stationary state. Identification of the regularities in the transient mode offers the possibility to gain an insight into the character and specific features of the key properties of the medium and its physical mechanisms, which govern the dynamics of the seismicity (Pandey and Chadha 2003, Singh *et al*. 2008, Abe and Suzuki 2012, Vallianatos *et al*. 2012).

In a case of induced seismicity we have some information about the origin of initiation and can claim with certain limitation about reproducibility of field experiments. Field experiments for initiation of seismicity by injection of the water in boreholes are carried out in special test sites generally for investigation of rock permeability. Data of these experiments allow to study such key questions as regularities and physical mechanisms of seismicity generation, local stress field disturbance and evolution, failure front spreading (*e.g.*, Horálek and Fischer 2008, Shapiro *et al.* 2007, Shapiro and Dinske 2009, Dahm *et al*. 2010, Fischer *et al*. 2008, Fischer and Guest 2011, and references therein).

Laboratory modeling of the transient modes of seismicity was carried out previously by the authors of this paper (Smirnov and Ponomarev 2004, Ponomarev *et al.* 2008). The step-like load regime was used to investigate the regularities and patterns of acoustic emission response structure under different strain rate of step. The experiments proved that step-wise initiation may induce transition processes similar to natural phenomena, *i.e*., seismic swarms and aftershocks. The nature and parameters of acoustic activity that reflects an intensity of the failure process vary with the increasing of the stresses and, correspondingly, with oncoming of the state of the specimen to the critical state.

Field experiment for seismicity initiation by the water injection in the borehole, conducted in the Soultz-sous-Forêts site in 1993 had step-like in-

jection history similar to our laboratory experiments. Results of analysis of data of this field experiment are presented in this paper.

2. SOULTZ-SOUS-FORÊTS FIELD EXPERIMENT

The experiment was carried out in the European Communities hot dry rock test site Soultz-sous-Forêts. The detailed description of the year 1993 experiment and original data are presented in (Cornet *et al*. 1997, Evans *et al*. 2005a, b, Evans 2005, Gerard *et al*. 2006).

The experiment consisted of injecting water into the borehole 3600-m deep (GPK1), which induced the local seismicity registered by a special network. The casing shoe of the borehole was located at a depth of 2850 m; and the remaining 750 m of this well were an open hole 6.25 inch (15.88 mm) in diameter. The borehole penetrates the granite crystalline basement at a depth of approximately 1400 m. Preliminary hydraulic testing under low water pressures revealed that the rock permeability is small everywhere near the borehole except for the zone of fracturing, which crosses the hole at a depth of 3490 m. During the experiment discussed here, the well was filled with sand within the depth interval of 3400-3600 m, in order to exclude the intense water discharge through the weakened fractured zone.

Water injection was executed in several stages: in August, September, and October 1993. At the first stage, the volume of injected water was small, and this stage represents no value for this work. Hydraulic rupturing occurred at the last stage (October 1993); this stage is also omitted from consideration. The largest volume of water (25 000 m^3) was injected into the hole at the second stage (September 1993). Water was injected stepwise during 17 days, with the fixed injection rate ranging from 0.15 to 36 l/s (Fig. 1). According to Evans (2005) and Evans *et al*. (2005b), the latter exhibits no significant vertical variations within the open part of the well. The rock pressure at a depth of 2805 m was 28.4 mPa.

Evans (2005) and Evans *et al*. (2005b) report on the general properties of seismicity and the structure of the fracturing caused by water injection. The main results of their studies are given below:

- A cloud of earthquakes 0.5 km wide, 1.2 km long, and 1.5 km thick is oriented at 225°NW. One of the most significant structures of the cloud extends downward by 350 m from the water injection point. This structure appeared at the initial stage of injection and likely reflects the main channel of the water drainage from the injection area. This structure is formed by near-vertical strike-slip fractures oriented in the NNW-SSE direction and forming a fault zone 10-20 m wide. This structure probably existed at that place even before the experiment, and its permeability increased due to water injection.

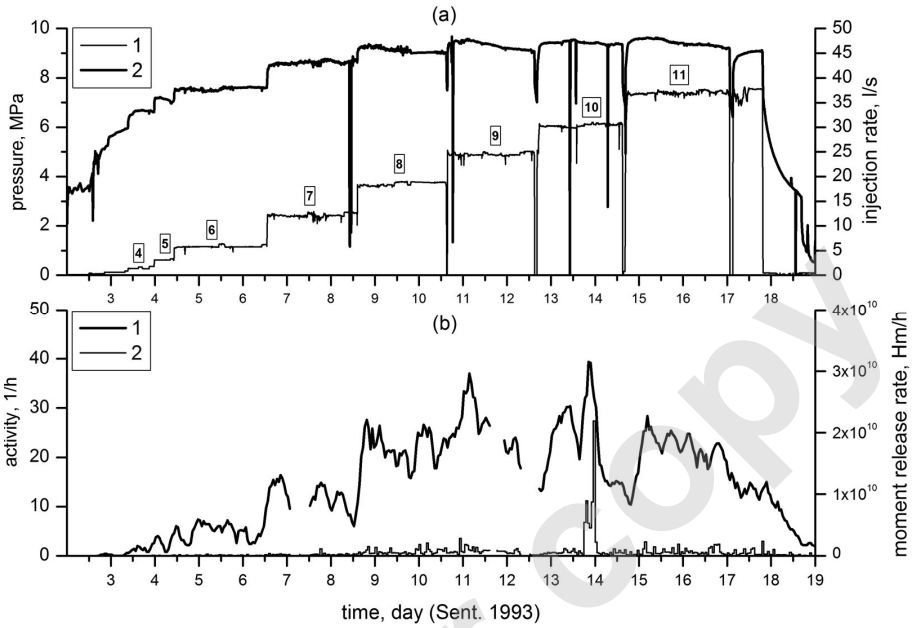

Fig. 1. History of water injection: (a) Water injection rate (1), and the downhole pressure excess above ambient formation pressure (differential pressure in terms of Evans *et al*. (2005b)) (2); series numbers are indicated near the curve of the water injection rate; (b) Parameters of induced seismicity: (1) activity (number of seismic events per hour), (2) rate of the seismic moment release.

- Regular logging measurements during the experiment revealed six zones of enhanced permeability, located at different depths in the open part of the hole.
- The analysis of the field of stress indicates that the pore pressure up to a depth of 2900 m (the uppermost part of the open hole) exceeds the minimal horizontal compression beginning from the water injection rate of 18 l/s. For deeper layers, the pore pressure is lower compared to the value of minimal compression. This peculiarity is reflected in the structure of seismicity (and, correspondingly, in the pattern of fracturing). Above 2900 m, the cloud of seismicity extends in the S-N direction, which corresponds to the direction of the axis of stresses; *i.e*., the structure of the failure is controlled through the jacking stress. Below 2900 m, the seismicity strikes NNS and corresponds to the orientation of the strike-slip fractures that existed prior to the experiment. In this case, the structure of the failure suggesting geological structure control through shearing.

- The seismicity and, correspondingly, the process of fracturing migrate with time downwards, which cannot be explained by purely hydrostatic factors, since the pore pressure is lower as compared with the minimal compressing stress. Based on the previous models suggested for the swarms of volcanic earthquakes (Hill 1977), Evans (2005), and Evans *et al*. (2005b) explain this phenomenon by the dynamics of the seismicity itself: the dilatancy-related opening of the strike-slip ruptures, their influence on the neighboring cracks, and thus the formation of the vertical channel. In fact, here, we are dealing with the propagation of a certain wave of relaxation oscillations similar to the "domino effect", self-oscillations in the active media, or the waves of seismicity.

Prior to the experiment, the medium in the region of the borehole was possessed of a system of different-scale defects. Water injection stimulated the development of this system due to the fracturing of its elements. Thus, water injection does not form a new system of fracturing but acts as an external factor, which triggers the evolution of the existing complex system of heterogeneities (defects) in the geological medium.

3. ORIGINAL DATA

Seismic events during the experiment of 1993 were registered by three four-component accelerometers installed within three abandoned oil wells and by the hydrophone in the borehole EPS1. The aperture of the network was 2 km (the observation wells are located at distances of 0.5 to 1.54 km from the borehole GPK1). The frequency band of the equipment was from 10 to 2500 Hz, and the sampling frequency was 5 kHz. The initial errors of the location of the hypocenter are 20 m in the vertical and 50 m in the horizontal directions. For increasing the resolution, special algorithms were applied. The algorithms are based on the combination of data for groups of events with similar wave characteristics (multiplets). This allowed the location error to be reduced by an order of magnitude. There are intervals of data loss due to the damage of the magnetic tape at the injection "steps", corresponding to water injection rates of 12 and 24 l/s. The seismic catalogue contains information about the time, the coordinates, and the moment magnitudes of earthquakes.

Figure 1 illustrates the original data. Let us term the data corresponding to the water injection "steps" as series. The series numbers and the water injection rates are indicated in Fig. 1. No seismic events have been observed for the first three series; therefore, they are omitted from further discussion.

Water injection and pressure. Figure 2 presents the scatter plot of the water injection rate Q and pressure P. Beginning from $Q = 18$ l/s (8th series in Fig. 1), the pressure increasing with the increasing rate of water injection

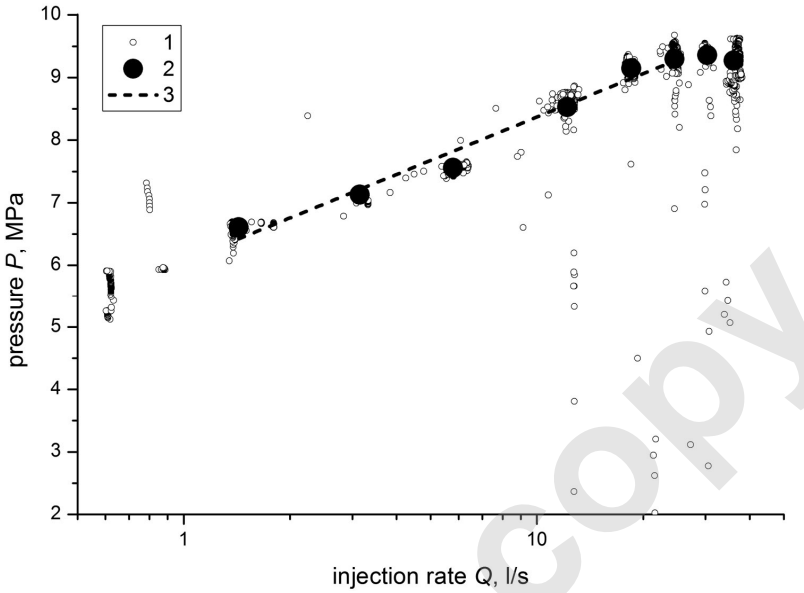

Fig. 2. Water injection rate and pressure: initial data (1), average over series (2), and approximation $Q \sim e^{\beta P}$ (3).

practically ceased. Evans *et al*. (2005a) explain this phenomenon by the increased permeability of the rock due to the development of the failure: it should be noted that according to the estimates by Evans (2005) and Evans *et al*. (2005b) the pore pressure becomes equal to the minimal compressing stress in the upper part of the open hole segment precisely at $Q = 18$ l/s.

As follows from Fig. 2, at $Q \le 18$ l/s , the dependence between P and Q approaches the linear one in semi-logarithmic scale. This means that in this interval $Q \sim e^{\beta P}$. If the permeability is assumed to be proportional to the fracturing of the rock material, such an exponential dependence is consistent with the notions of the kinetic concept of failure (Zhurkov 1965). Indeed, according to Zhurkov's formula, the probability of failure is proportional to $e^{\gamma\sigma}$. Additional stresses σ induced by the water pressure should naturally be considered as being proportional to P: $\sigma = \alpha P$. The fracturing is evidently proportional to the probability of failure; it means that this quantity, as well as the permeability Q will be proportional to $e^{\gamma\sigma P}$, which is illustrated in Fig. 2.

Completeness magnitude of catalogue. Approaches to evaluation of a magnitude of completeness are based on the proposition of the power law of earthquake distribution on energy, and in this case, the frequency-magnitude relation is linear (Wiemer and Wyss 2000 and references therein).

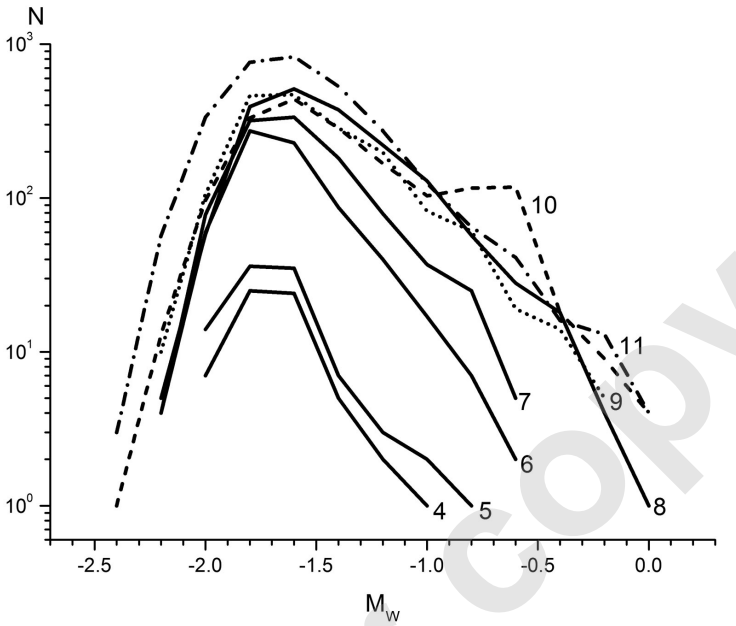

Fig. 3. Frequency-magnitude diagrams for different series (series numbers are indicated near the curves).

If some earthquakes are missing, points for corresponding magnitude will be located below the frequency-magnitude straight line, which determines the "fall-off" of the FM-relation at small magnitudes. Therefore, the problem of finding a completeness magnitude in terms of statistics comes down to the problem of consistency of observed earthquake distribution on energy with power law distribution. Pisarenko (1989) found a strict statistical solution to this problem, which makes it possible to carry out the analysis by simply setting the significance level for verification of relevant hypotheses.

The analysis of temporal variations of the completeness magnitude revealed that the threshold for the data selection should be taken as $M = -1.6$. The analysis of the spatial distribution of the magnitude of completeness shows that this value is actual for the main cloud of seismicity.

Figure 3 presents the plots of the frequency-magnitude relation calculated separately for all the series. It is seen that the above estimate of the completeness magnitude is valid for all the series.

4. STATISTICAL PARAMETERS OF SEISMICITY

To analyze the variations of seismicity, a number of statistical parameters were estimated in the moving time windows. These parameters are described

below, and those of them which are uncommon are considered in more detail.

***b*-value:** The maximum likelihood estimate (MLE) for a non-grouped sample was used for Gutenberg–Richter *b*-value (Aki 1965),

$$b = \frac{\log_{10} e}{\bar{M} - M_0} \ ,$$

where $\bar{M}$ is the average magnitude, and M_0 is threshold magnitude. The uncertainty S_b of *b*-value is determined as the root of its estimated asymptotic variance, equal to b^2/N: $S_b = b/\sqrt{N}$, where N is number of events.

***d*-value:** The fractal dimension of seismicity is most often estimated using correlation integral technique,

$$C(R) = \frac{n(\Delta r \le R)}{N(N-1)/2} \ ,$$

where $n(\Delta r \le R)$ is the number of pairs with a distance smaller or equal to R, N is total number of earthquakes (see Kagan (2007) and references therein). For the fractal set $C(R) \sim R^d$, where d is correlation fractal dimension. This technique is based on the set of distances between all possible pairs of events, *i.e.*, deals with fairly large data sets. The number of possible pairs in a catalog of N events is $N(N-1)/2$, ensuring the stability of an estimate with only hundreds or even tens of earthquakes available from a catalog resulting in not only increased computation time but also complicated estimation of the correlation dimension uncertainty. The interdependence of $N(N-1)/2$ distance pairs derived from N events complicates the estimation of correlation integral asymptotic variance and requires the introduction of corrections for a correlated sample (Pisarenko and Pisarenko 1995). We used a direct estimation method to obtain an approximate estimate of its variance. This method, known as "jackknife", is based on the influence function approach (Huber and Ronchetti 2011, Mosteller and Tukey 1977).

***q*-value:** The Gutenberg–Richter law and fractal geometry of seismicity reflect such a basic property of the fracture process as its self-similarity. The former can be related to the statistical distribution of earthquake source sizes and shows how the number of events decreases with increase in their value (magnitude, seismic moment, or other characteristic of this type). The latter can be related to the distribution of distances between sources and shows how the number of events in a spatial region increases with an increase in its size. Both relations are unified into the Generalized Gutenberg–Richter law or Unified scaling law for earthquakes (Kosobokov and Mazhkenov 1988, 1994, Keilis-Borok *et al.* 1989, Chelidze 1990, Bak *et al.* 2002).

$$\log N = -b \log E + d \log L + \text{const} \ ,$$

where N is the number of earthquakes having the energy E that occurred in an area of the size L over time T. This law inter-relates statistical estimates obtained in areas of various sizes from sets of events of various energies. In this way, seismic statistics can be reduced to the source region and estimates obtained from this statistics can be compared to parameters of fracture physics.

Using the unified scaling law, the duration of the fracture cycle of lithosphere material can be estimated from data of an earthquake catalog (Smirnov 2003). The duration of the fracture cycle is understood as the time interval equal to the inverse of the average recurrence rate of earthquakes of a given magnitude in a region equal in size (l) to the earthquake source. The following expression obtained for the average duration of the fracture cycle:

$$\tau(l) = \tau_0 \left(l / l_0 \right)^q \ ,$$

where τ_0 is the cycle duration determined for events of the size l_0, $q = \alpha b - d$, and the coefficient α relates the magnitude scale in use to the source size: $M = \alpha \log l + \beta$. Parameters q (q-value) and τ_0 can be estimated from earthquake catalog data (Smirnov 2003).

The q-value indicates the dependence of fracture cycle duration on earthquake source size (or on magnitude). Results obtained in Smirnov (2003) indicate that, in the background regime, the fracture cycle duration weakly depends on the magnitude (the parameter q is close to zero), implying that the fracture process on various scales (presented by source sizes of earthquakes considered) develops at approximately the same rate. If $q < 0$, then failure is more intensive on higher scales. This situation is typical of the initial stage of aftershock sequences; over time, q-value in aftershock sequences increases returning to its background value (Smirnov and Ponomarev 2004). This indicates that aftershock relaxation follows the so called "direct cascade" scenario which involves redistribution of intensity of a relevant process (in this case, failure process) from higher scale levels to lower scale levels. q-value decreasing from positive values to zero corresponds to inverse cascade, *i.e.*, gradual transition of the failure process from lower to higher scales. Among other factors, it corresponds to the scenario of fracture growth resulting from their interaction and, therefore, gradual transition of failure to higher scale levels, which is reflected in the avalanche-unstable fracturing concept.

5. DYNAMICS OF SEISMICITY

As an estimate of the effective radius of the seismically active area the so-called radius of gyration was used. The gyration radius is the root-mean-

square of the distances between events and the barycentre of the events cloud (the barycentre is a point, whose coordinates are the average coordinates of the hypocenters of events in the earthquake cloud). The following scenario of selection was applied in the eventual calculations: for each series, its own sphere was taken with the center in the barycentre of the cloud of the series and the radius equal to the radius of gyration.

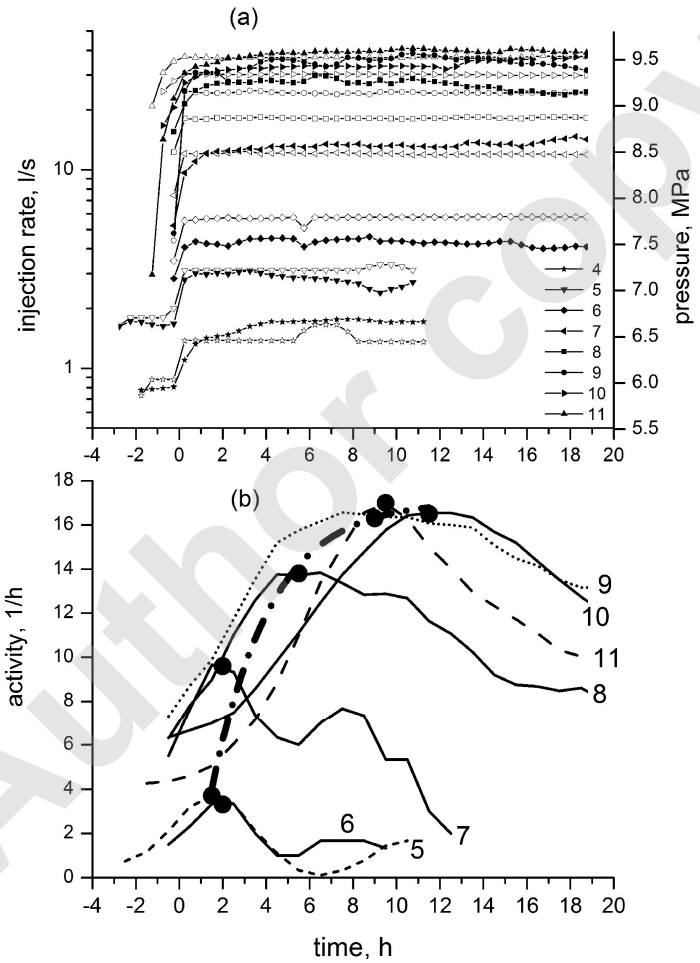

Fig. 4. Water injection and seismic activity: (a) variations of the water injection rate (open symbols) and differential pressure (solid symbols) for different series; (b) variations of the seismic activity for different series for selected data (a separate sphere for each series with the radius equal to the gyration radius and the center in the barycentre of the cloud of seismicity of the corresponding series); series numbers are indicated near the curves. Solid dots indicate the maxima of seismic activity for each series.

Figure 4 shown variations of the seismic activity for each series. In addition to the expected increase in activity at the transition to higher rates of water injection, the delay of the maximum activity relative to the beginning of water injection into the borehole is seen in the figure. It is also clearly seen that the higher the number of the series, the longer is the delay: the peak activity shifts to the right along the time axis. The duration of increasing of the water injection rate did not exceed one hour. The delay of the seismic response is substantially longer and, consequently, cannot be explained by this factor. The delay exceeds also the typical time of pressure stabilization for the new level of injection rate.

To study the possibility for the influence of the selection rules to the delay of the seismic response curves being analogues to presented on Fig. 4 was calculated for different scenario of selection. The following selections for series data were considered: without selection; for all the series, a sphere with a radius of 150 m and the center in the barycentre of the cloud of seismicity; for each series, its own particular sphere with a radius of 150 m and the center in the barycenter of the corresponding series. The obtained results are presented in Fig. 5 as the dependences of the delays of peak seismic re-

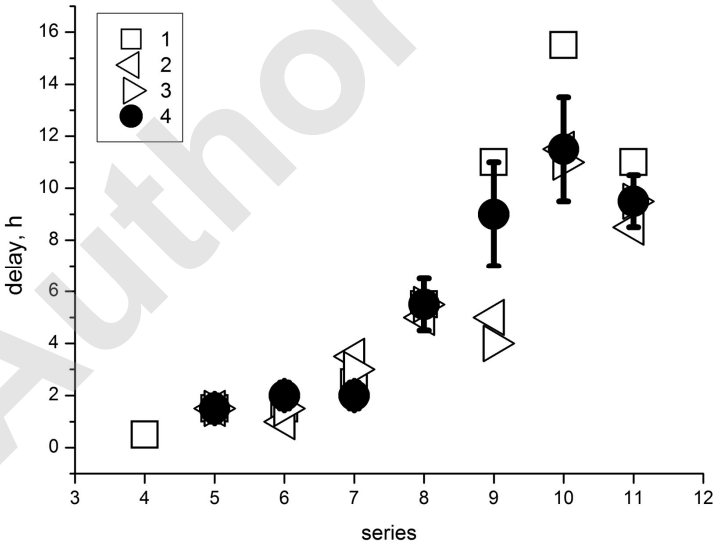

Fig. 5. Delays of the seismic response for different variants of selection: without selection (1), the same sphere for all series with the radius of 150 m and the center in the barycentre of the cloud of seismicity (2), a separate sphere for each series with the radius 150 m and the center in the barycentre of the cloud of seismicity of the corresponding series (3), and a separate sphere for each series with the radius equal to the gyration radius and the center in barycentre of the cloud of seismicity of the corresponding series (4).

sponses on the series number. It is seen that regardless of the selection scenario, the delay increases with the series number, and the delays corresponding to different selections are close to each other. This allows eliminating the spatial selection as an artificial factor, responsible for the delay of the seismic response, but the physical dependence of the delay on the size of the seismically "excited" area is possible.

The delay of peak activity for chosen selection (Fig. 4) is given as a function of the pressure of the injected water in Fig. 6. The abscissa axis indicates the values of pressure for the preceding series, *i.e.*, the pressure under which the seismic activity was excited by water injection. The growth of the delay with increasing pressure (*i.e.*, with the enhancement of acting local stresses) is shown in Fig. 6. It should be noted that when the pressure exceeds the value of the minimal tectonic compression in the upper part of the open borehole segment (let us recall that the pressure reaches this value at the step of the 8th series under $Q = 18$ l/s, Fig. 1), the delay in the seismic response remains practically the same (last three points in Fig. 6).

To obtain information about the pattern and probable dynamics of the failure process, we have estimated statistical parameters of seismicity for each series. Figure 6 displays the estimates of *b*-, *d*-, and *q*-values (in the calculations of the latter parameter it was taken that $\alpha = 2$, according to the type of the moment magnitude used in the catalogue). Figure 6 presents the

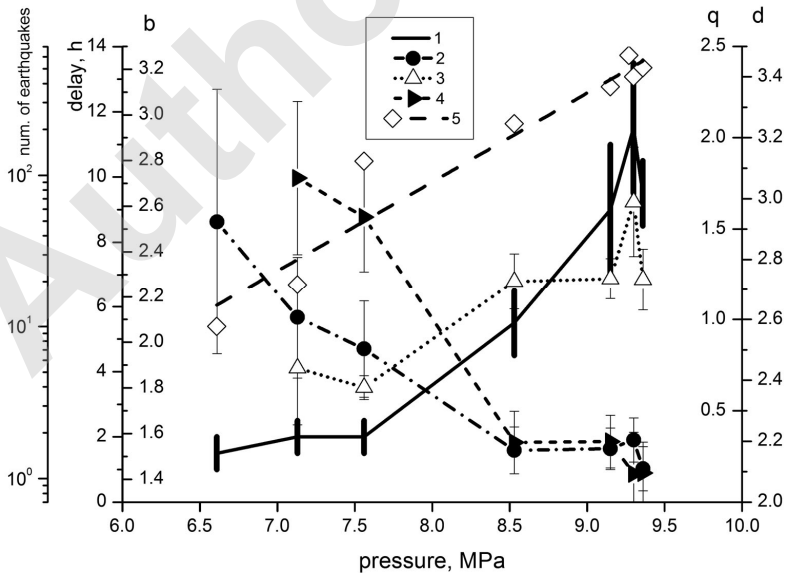

Fig. 6. Statistical parameters of seismicity as function of the water pressure: (1) delay of the seismic response, (2) *b*-value, (3) *d*-value, (4) *q*-value, (5) total number of earthquakes in series; the straight line – exponential approximation.

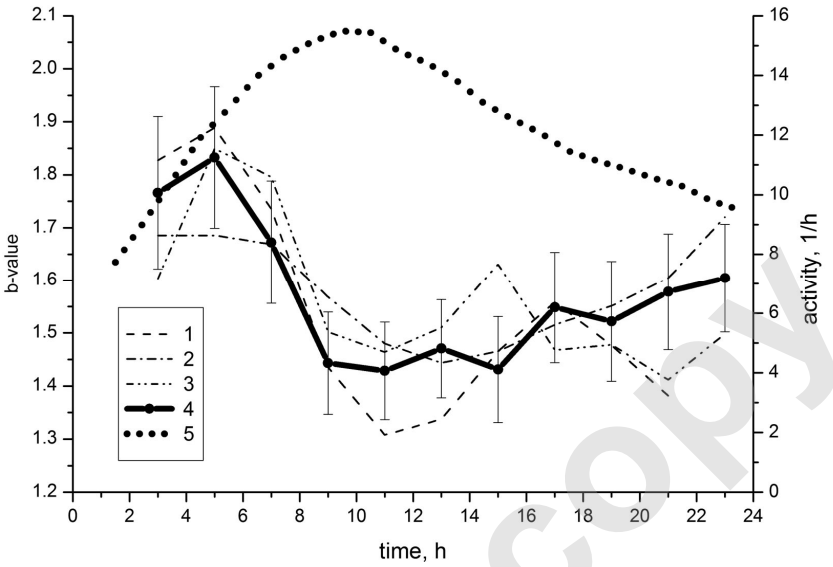

Fig. 7. Time variations of *b*-value within series: (1) 9th, (2) 10th, and (3) 11th; (4) average *b*-value for three series, and (5) average activity for three series.

total number of earthquakes in each series too. The dependence of the number of events on pressure is well approximated by the exponent.

Figure 7 presents the temporal variations in *b*-value averaged for the last three (9-11) series; for the earlier series, the statistics of events is insufficient for the study of temporal variations in *b*-value. Figure 7 demonstrates the tendency of variations: at the stage of increasing seismic activity *b*-value decreases, while at the stage of a decreasing of activity, it increases.

6. MULTIPLETS

Bourouis and Bernard (2007) revealed and analyzed the groups of earthquakes called multiplets. Each multiplet includes events with similar waveforms (the coefficient of correlation of waveforms exceeds 0.9). Analysis of waveforms for all events in the multiplet as a whole allows to increase significantly the accuracy of their location. The authors of the cited work interpret each multiplet as the repeated acts of fracturing of the same asperity. The source spectra of the events of each multiplet are similar in shape but different in amplitudes; correspondingly, the events of the multiplet have different magnitudes. The temporal distribution of the events within the multiplet obeys Omori's law (at least at the initial stage), which confirms the idea of the consideration of multiplet events as a realization of the failure process of the "excited" asperity.

The catalogue of multiplets contains information about 4825 events that form multiplets each consisting of 2 to 75 events and 4334 singlets (the events that do not enter into any multiplet).

If each multiplet is considered as a manifestation of the process of the asperity fracturing, it is possible to estimate the size of the asperity from the multiplets. The gyration diameter $D_g = 2R_g$ defines the area that includes (in case of the Gaussian distribution) approximately 66% of events, and the doubled gyration diameter, 96% of events. Let us take the latter value as an estimate for the size of the asperity: $L_a = 2D_g$. We consider L_a estimates as being preferable because they are statistically more stable compared to the frequently used estimates of the "maximal diameter": the latter are based in fact on a single point determinations (the event located at the maximal distance from the barycenter), while L_a is estimated from the entire set of data.

Figure 8 illustrates the distribution of asperities on sizes L_a. For comparison, also the magnitude distribution of all the registered earthquakes (singlets included) is presented. In the abscissa axis, the scale of magnitudes is combined with the scale of the heterogeneity sizes according to the relation $M_w = 2 \lg L_a(M) - 1.92$. This relation agrees well with both the magnitude and energy estimates of the focal sizes of earthquake (Abercrombie *et al*. 2000, Bormann 2002, Smirnov 2003).

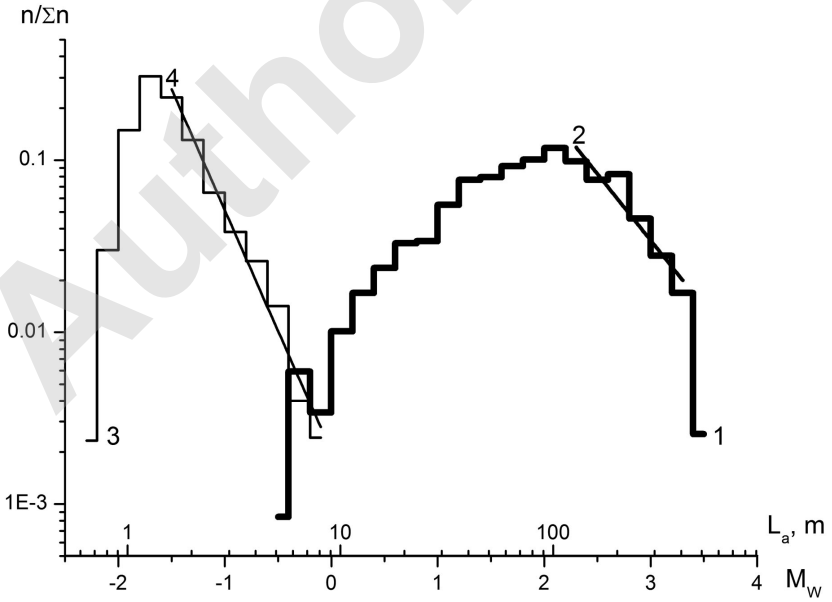

Fig. 8. The distributions of asperities on size (1) and earthquakes on magnitude (3); power law approximation of the descending branch of the asperity distribution (2); and the Gutenberg–Richter law approximation for earthquake distribution (4).

7. DISCUSSION

A. Dependence of statistical parameters of seismicity on the level of local stress caused by the injected water pressure was illustrated in Fig. 6. Main results are exponential increasing of total number of earthquakes per series, and decreasing of *b*- and *q*-values.

Exponential dependence of activity on the stress is in agreement with the kinetic concept of the strength of solids (Zhurkov 1965), or stress corrosion in other terms. Zhurkov's formula for the material durability

$$\tau = \theta_0 e \frac{U_0 - \gamma\sigma}{kT} ,$$

(where θ_0 – period of thermal oscillation, U_0 – activation energy, γ – so named structure-sensitive parameter) is in essence the Boltzmann exponent. The value inverse to the durability determines the probability of failure; therefore, in the context of the kinetic concept, the exponential dependence of the number of failure acts during a certain time interval on the applied stresses should be expected.

Decreasing of *b*- and *q*-value with local stress increasing indicates the evolution of the failure process on scales. Decreasing of these parameters demonstrates increasing of the part of relatively strong seismic events. The explanation of this phenomena is well known in terms of crack fusion and growth or two-stage model of fracture of rocks and the avalanche-unstable fracturing scenario for seismicity (Mjachkin *et al*. 1975, Chelidze 1986, Enescu and Ito 2001, Bachmann *et al. 2*010, Sobolev 2011, Reches and Lockner 1994, Chelidze *et al*. 1994, Zavyalov 2002, Lei *et al*. 2003). The frequency-magnitude diagrams (Fig. 3) confirm this inference. This figure shows that the lower series are lacking in relatively strong events, which appear gradually in the higher series. Similar results were obtained in the laboratory experiments (Ponomarev *et al*. 1997) with the gradual formation of the macroscopic zone of failure.

The anomalously high (for the usual background seismicity) value of $b \approx 1.4$, observed in the last series, indicates that the process of the formation of the seismogenic structure, typical for the background seismicity of tectonically active regions, has not been completed in the conducted experiment. This conclusion can be confirmed by analysis of the asperity size distribution.

The size distribution of the asperities (Fig. 8) is similar to the typical distributions of lithosphere heterogeneities of different scales: faults, crustal blocks, lithosphere plates, *etc*. (Cladouhos and Marrett 1996, Nicol *et al*. 1996, Watterson *et al*. 1996, Yielding *et al*. 1996, Bird 2003, Sornette and Pisarenko 2003, Goto and Otsuki 2004). The power-law approximation of

the descending branch of the distribution $\lg N = -d_a \lg L_a + \text{const}$, based on the concept of self-similarity of the lithosphere heterogeneities, yields the estimation of the self-similarity exponent as $d_a = 1.6$. This value, recalculated into the seismological "units" via a formal transition from L_a to M_w, provides the b-value of the "frequency-magnitude" relation with respect to asperity $b_a = 0.8$. This is close to the typical world-wide average value 0.9 for the Guttenberg–Richter parameter, although substantially lower than the b-value for the seismicity induced by water injection that changes from 2.5 at the beginning to 1.4 at the end of the experiment.

The interrelation between the exponents of the energy self-similarity of seismicity and geometric self-similarity of lithosphere heterogeneities is the subject of long discussion (Aki 1981, King 1983, Turcotte 1992, Bak *et al*. 2002, Corral 2005). The known relation $b = d/\alpha$ may be considered as the result of a certain consistency between the structure of the failure and the structure of the heterogeneities of the medium, when the energy distribution of earthquakes is entirely controlled by the size distribution of the heterogeneities. In this case, the probability of the failure of different-size heterogeneities proves to be constant. Such a situation is typical for the background seismicity, but is sharply violated in transient modes (Smirnov 2003, Smirnov and Ponomarev 2004). If we take the estimate d_a as the estimate of the self-similarity exponent for the structure of heterogeneities in the aria of the experiment, the relation $b = d/\alpha$, in our case, also becomes disturbed: even the minimal value of $b = 1.4$ reached at the end of the experiment is too high as compared with $d/\alpha = 0.8$ (α in our case is equal to 2). It indicates that transient process is not finished.

The laboratory studies show that the high b-values and, correspondingly, the "deficiency" of strong events are typical for the beginning stage of the formation of the failure zone (Zhurkov *et al*. 1977, Main *et al*. 1989, Ponomarev *et al*. 1997, Scholz 2002). The subsequent gradual grows of cracks due to their interaction (when the stress fields overlap near the tips of cracks) and their fusion is accompanied by the transition of failure from lower to higher scales, the appearance of successively stronger events, and decreasing of b-value. In the considered field experiment we observed the same situation: b-value decreases with the development of failure initiated by water injection, although it remains above the level corresponding to the structure of the medium heterogeneity (asperity system). This can be interpreted as an indication of the fact that the structure of fracturing had not matured completely during the experiment: the water pressure and, probably, the duration of injection (according to theoretical results of Shapiro *et al*. (2007), and Shapiro and Dinske (2009)) are likely insufficient for the evolution of the experiment area into the state typical for tectonic regions with well-developed background seismicity.

B. Figure 7 demonstrates time variations of *b*-value for series of initiation: *b*-value increases on the stage of activation and decreases on the stage of relaxation. The statistical significance of variations of *b*-value is not high; however, the revealed tendencies allow suppose that the excitation is implemented through the transition of fracturing from lower to higher levels; and the relaxation, through the transition from higher to lower levels.

The decreasing of *b*-value with time is typical for process of earthquake preparation (Zhang and Fu 1981, Smith 1981, Main *et al*. 1989). This decreasing is explained as result of the gradual redistribution of fracturing on scales, which develops from lower to higher scales (Sobolev 2011 and references therein). Increasing of *b*-value is typical for relaxation of the seismic activity in aftershock sequences. It indicates that the relaxation is accompanied by both a decrease in the seismic activity and the scale redistribution of the failure processes. Smirnov and Ponomarev (2004) shown that immediately after the main event the failure processes are focused mainly on large-scale events, whereas during the relaxation it involves smaller events, eventually returning to the distribution typical for the background seismicity. Figure 7 indicates that in our case of water injection initiation the excitation and the relaxation probably develop by the same scenarios.

C. Figures 4-6 demonstrate the delay of seismic response to the water injection. This delay is different for different series: the stronger the local stresses caused by the injected water pressure, the later the activity reaches maximum and the relaxation (the decay of the activity) begins. This delay can be explained by some kinetic process, such as water diffusion in porous medium or failure front spreading. Both process results in the increasing of seismogenic area, the nature and the mechanisms responsible for this increasing are of significant importance for the problem in question. Does failure precede the penetration of water that fills the fractured areas of the medium; or, on the contrary, the failure follows the front of water diffusion? In fact, this is the question about the nature of development of seimogenic area: is one controlled by the kinetics of the failure itself, or does it simply reflects the kinetics of water propagation? And if both mechanisms work, how can the contribution of each mechanism be estimated?

Shapiro *et al.* (1999) analyzing data of the same experiment in Soultz-sous-Forêts approximates the increase in the size of the area of induced seismicity R with time t as normal diffusion: $R = \sqrt{4\pi Dt}$. This approximation is derived from the dependence of the maximal distance between the water injection point (the lower, open part of the borehole) and the hypocenters of induced earthquakes on the time after the beginning of the experiment. The following issues emphasized by Shapiro *et al*. (1999) are of principal significance for us. The stresses caused by both the water injection

and aseismic displacements propagate faster than the front of the water diffusion. These stresses cause earthquakes (we mean the triggering mechanism) in the as yet unfractured area, thus forming the wave of fracturing, which propagates ahead of the wave of the pore pressure.

In order to form our own view to increasing of the fracturing area and its consistency with the diffusion model, we analyzed the growth of the seismogenic area with time. We used the catalogue containing only earthquakes of magnitude within the range of completeness (in Shapiro *et al*. (1999), the question of catalogue completeness remained beyond the discussion). To characterize the size of the seismogenic area, we used the radius of gyration with respect to the barycenter of the cloud of earthquakes within each time interval, instead of the maximum distance of earthquakes from the water injection point used by Shapiro *et al.* (1999). As mentioned above, the radius of the gyration is more stable statistic estimate. The fixed position of the "center of diffusion" in the point of the borehole seems disputable, since in the course of the development of fracturing the water may be injected from other points through the formed channels of enhanced permeability – the "center of diffusion" may migrate within the fractured area (Cornet 2000).

For the convenience of comparison, let us assume that the radius of the cloud relative to its barycenter is $R = 2R_g$. The time dependence of R is shown in Fig. 9a. This figure presents also the distances between the borehole and the hypocenters of earthquakes – by analogy with Shapiro *et al*. (1999), and the distances between the borehole and the barycenters of the clouds of earthquakes. The figure reproduces also the diffusion curve with coefficient $D = 0.05$ m^2/s after (Shapiro *et al*. 1999). Figure 9a is similar to Fig. 1 from the latter work, and the diffusion approximation of the maximum distances between the borehole and the hypocenters of earthquakes seems at first sight acceptable.

More detailed information about the relation between the size of the seismogenic area and time can be obtained from Fig. 9b, where the same data as in Fig. 9a are presented in bi-logarithmic scale. It is seen here that at the beginning of the experiment, within approximately the first 100 hours, the displacement of the barycenter of the cloud of seismicity is comparable with its size. It means that the model with a single point of diffusion center is inexact within the period of the first 100 h (which is emphasized in Cornet (2000)). During the period from 100 to 360 h, the normal diffusion approximation is not quite consistent with the observed data: the slope of the straight line (4) in Fig. 9b is larger than prediction of normal diffusion model. Thus, the normal diffusion can be considered only as a rough approximation for explanation of increasing of the seismogenic area.

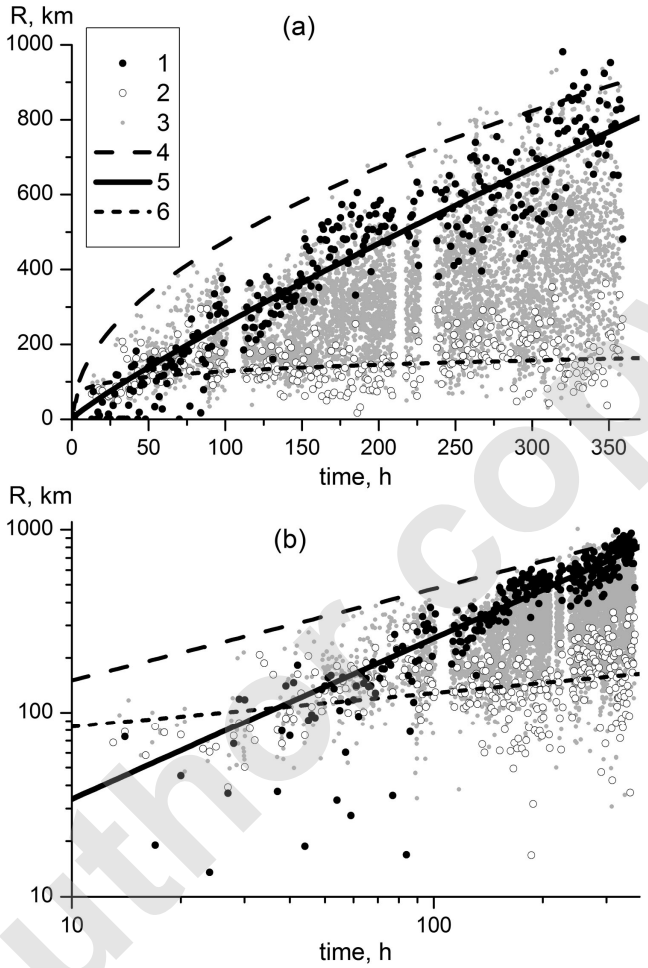

Fig. 9. The size of the cloud of seismicity as a function of time from the beginning of the experiment in the linear (a), and bi-logarithmic (b) scales: (1) size of the cloud estimated from the gyration radius, (2) distance from the borehole to the barycentre of the cloud, (3) distance from the borehole to hypocenters of earthquakes (by analogy with Shapiro *et al.* (1999)), (4) diffusion approximation $R = \sqrt{4\pi Dt}$ for $D = 0.05$ m^2/s after Shapiro *et al*. (1999), (5) power-law approximation of the size of the cloud, and (6) power-law approximation of the distance between the borehole and the barycentre of the cloud.

Figure 9 presents the power-law approximation obtained by the formal regression $\log R$ on $\log t$ within the interval from 100 to 360 h. The exponent c in relation $R = At^c$ is estimated equal to $c = 0.88 \pm 0.03$. This value is significantly more than 0.5, and is typical for super-diffusion (*e.g.*, Vlahos *et al*.

2008), which can be realized, for example, as non-linear diffusion with pressure-dependent diffusion coefficient (Shapiro and Dinske 2009).

In our opinion, the more intensive growth of the seismogenic area than that for normal diffusion can be considered as indicator of the other mechanism of the development of the fractured area, which acts solely or in addition to the hydrodynamic one (the last case corresponds to the non-linear diffusion). The kinetics of fracturing may be such a mechanism; the specific example for considering experiment is discussed in Evans *et al.* (2005a, b), Evans (2005), and Bourouis and Bernard (2007).

Diffusion-like space-time patterns are known for natural seismicity induced by different impacts, as possibly related with water presence (Noir *et al.* 1997, Daniel *et al*. 2011), and without special consideration of water influence (Marsan *et al*. 2000, Huc and Main 2003, Helmstetter *et al*. 2003) as well. The possibility of the diffusion-like spreading of the fracturing area without of liquid diffusion is confirmed in the laboratory experiments. The results obtained in one of such experiments conducted in the Rock Friction Laboratory (USGS) are presented below. The data obtained in a series of experiments, including the one mentioned above, were analyzed many times (Lockner *et al*. 1991, 1992a, b, Lockner 1993, Lockner and Stanchits 2002, Reches and Lockner 1994, Ponomarev *et al.* 1997). These works provide a detailed description of the instrumentation and technique used in the experiment (in the last two works, the experiment under consideration is designated as AE42).

A dry Westerly granite specimen was subjected to uniaxial loading under uniform compression (under confining pressure). The special system of sensors mounted on the specimen allowed locating the sources of the acoustic emission and compiling the catalogue of acoustic events, similar to the catalogue of earthquakes. A special regime of loading under the acoustic emission rate feedback control made it possible to conduct a detailed study of the nucleation and development of the fracturing area.

Until a certain stage, while the distances between the microcracks substantially exceed their sizes, fracturing is uniformly distributed throughout the specimen. With the increase in the density of microcracks, the distances between them decrease, and the stress fields concentrated at the tips of cracks become overlapping, which leads to the interaction of the cracks. This results in the transition of the failure into the stage of localization: a small area (the "nucleus" of the macroscopic facture) is formed inside the specimen, where the process of fracturing is concentrated; the acoustic activity outside this area sharply decreases (Mjachkin *et al*. 1975, Chelidze 1986). Then, the size of the "nucleus" area gradually increases: as the failure develops, this area grows forming a narrow zone close to the plane of maximum Coulomb stresses. The regime of loading is such that this growth occurs un-

der stresses nearly constant in time. If the loading continues, this narrow zone of failure crosses the entire specimen, thus, forming a macroscopic fault.

Figure 10 illustrates time dependence of the size of the fracturing area derived from the acoustic catalogue (the above-mentioned methods were

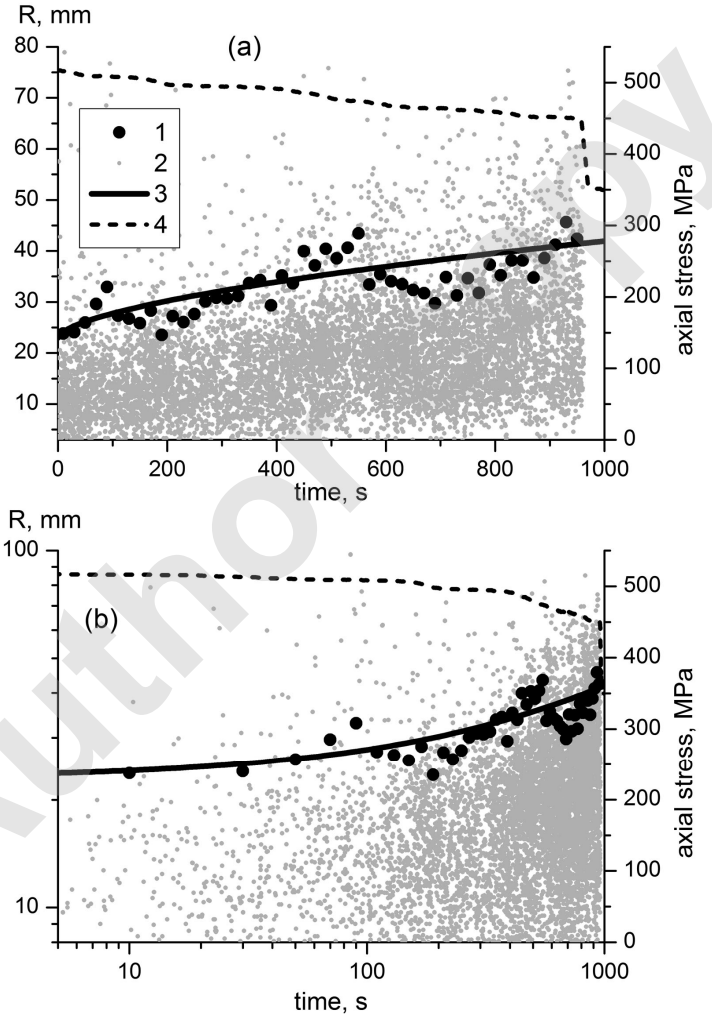

Fig. 10. The size of the cloud of acoustic events as a function of time from the beginning of nucleation in the linear (a), and bi-logarithmic (b) scales: (1) size of the cloud estimated from the gyration radius, (2) distance between the barycentre of nucleation and the hypocenters of the acoustic events, (3) power-law approximation of the size of the cloud $R = At^c + R_0$ (the initial size of the "nucleus" R_0 taken into account), and (4) axial stress of machine loading.

used). The regression $R = At^c + R_0$ yields the following estimates: $c = 0.6 \pm 0.2$, $R_0 = (23 \pm 7)$ mm (the summand R_0 is added to allow for the nonzero initial size of the "nucleus" failure area). Thus, the dynamics of the area of the failure is close to the normal diffusion, although it should be emphasized again that no liquid injection was used in the experiment. This example demonstrates that the kinetics of the failure process may provide the same statistical results as the fluid diffusion.

8. CONCLUSIONS

- Changes of the similarity exponents of induced seismicity (GR b-value and introduced by authors q-value) are found in the field experiment, conducted in the Soultz-sous-Forêts test site in 1993. b- and q-values decreases with development of induced failure. It indicates to the redistribution of the failure process on scales from lower to upper, corresponding to the scenario of crack fusion and growth.
- The value of $b \approx 1.4$, observed on the last stages of field experiment, is anomalously high in comparison with values typical for the usual background seismicity. It indicates that the process of the formation of the seismogenic structure, typical for the background seismicity of tectonically active regions, has not been completed in the conducted experiment. This conclusion is confirmed by analysis of the asperity size distribution in comparison with earthquake size distribution.
- b-value varies in time within the series of the water initiation, reflecting the activation and relaxation of induced seismicity: b-value increases on the stage of activation and decreases on the stage of relaxation. These tendencies allow suppose that the excitation is implemented through the transition of fracturing from lower to higher levels; and the relaxation, through the transition from higher to lower levels.
- The total number of earthquakes per series of water initiation depends exponentially on the water pressure, and seismic activity reaches the maximum with delay from the beginning of initiation. The value of delay increases with the increasing of the initiating water pressure. It indicates to the kinetic nature of the excitation of the induced seismicity.
- The increasing in the size of the area of induced seismicity with time differs from the normal diffusion, caused by the water flow in the porous medium. Analysis carried out for the data of the laboratory experiment indicates that diffusion growth of the failure area may be realized in the dry specimen, without the fluid participation. In our opinion, both kinetic processes – water and the failure diffusion – can be significant for the development of seismicity induced by the water injection.

Acknowledgements. This work was carried out under financial support of the Russian Foundation for Basic Research, grants #11-05-00135 and #12-05-91051.

References

Abe, S., and N. Suzuki (2012), Aftershocks in modern perspectives: Complex earthquake network, aging, and non-Markovianity, *Acta Geophys.* **60**, 3, 547-561, DOI: 10.2478/s11600-012-0026-8.

Abercrombie, R., A. McGarr, H. Kanamori, and G. Di Torro (eds.) (2000), *Earthquakes: Radiated Energy and the Physics of Faulting*, AGU Geophysical Monograph Series, Vol. 170, 327 pp.

Aki, K. (1965), Maximum likelihood estimate of b in the formula log N = a – bM and its confidence limits, *Bull. Earthq. Res. Inst., Tokyo Univ*. **43**, 2, 237-239.

Aki, K. (1981), A probabilistic synthesis of precursory phenomena. **In:** D.W. Simpson and P.G. Richards (eds.), *Earthquake Prediction: An International Review*, Maurice Ewing Series, Vol. 4, AGU, Washington, D.C., 566-574, DOI: 10.1029/ME004p0566.

Bachmann, C., S. Wiemer, and J. Woessner (2010), The induced Basel 2006 earthquake sequence: Mapping seismicity parameters on small scales. **In:** *Abstract Book. The 32nd General Assembly of European Seismological Commission. Montpellier, France*.

Bak, P., K. Christensen, L. Danon, and T. Scanlon (2002), Unified scaling law for earthquakes, *Phys. Rev. Lett.* **88**, 17, 178501-178504, DOI: 10.1103/PhysRevLett.88.178501.

Bird, P. (2003), An updated digital model of plate boundaries, *Geochem. Geophys. Geosyst.* **4**, 3, 1027, DOI: 10.1029/2001GC000252.

Bormann, P. (ed.) (2002), *New Manual of Seismological Observatory Practice*, GeoForschungsZentrum, Potsdam.

Bourouis, S., and P. Bernard (2007), Evidence for coupled seismic and aseismic fault slip during water injection in the geothermal site of Soultz (France), and implications for seismogenic transients, *Geophys. J. Int*. **169**, 2, 723-732, DOI: 10.1111/j.1365-246X.2006.03325.x.

Chelidze, T.L. (1986), Percolation theory as a tool for imitation of fracture process in rocks, *Pure Appl. Geophys.* **124**, 4-5, 731-748, DOI: 10.1007/BF00879607.

Chelidze, T.L. (1990), Generalized fractal law of seismicity, *Doklady. Akad. Nauk SSSR* **314**, 5, 1104-1105.

Chelidze, T., T. Reuschle, and Y. Gueguen (1994), A theoretical investigation of the fracture energy of heterogeneous brittle materials, *J. Phys. Condens. Mat.* **6**, 10, 1857-1868, DOI: 10.1088/0953-8984/6/10/005.

Cladouhos, T.T., and R. Marrett (1996), Are fault growth and linkage models consistent with power-law distributions of fault lengths? *J. Struct. Geol*. **18**, 2-3, 281-293, DOI: 10.1016/S0191-8141(96)80050-2.

Cornet, F.H. (2000), Comment on "Large-scale in situ permeability tensor of rocks from induced microseismicity" by S.A. Shapiro, P. Audigane, J.-J. Royer, *Geophys. J. Int*. **140**, 2, 465-469, DOI: 10.1046/j.1365-246x.2000.00018.x.

Cornet, F.H., J. Helm, H. Poitrenaud, and A. Etchecopar (1997), Seismic and aseismic slips induced by large-scale fluid injections, *Pure Appl. Geophys*. **150**, 3-4, 563-583, DOI: 10.1007/s000240050093.

Corral, Á. (2005), Renormalization-group transformations and correlations of seismicity, *Phys. Rev. Lett*. **95**, 2, 028501, DOI: 10.1103/PhysRevLett.95.028501.

Dahm, T., S. Hainzl, and T. Fischer (2010), Bidirectional and unidirectional fracture growth during hydrofracturing: Role of driving stress gradients, *J. Geophys. Res.* **115**, B12, B12322, DOI: 10.1029/2009JB006817.

Daniel, G., E. Prono, F. Renard, F. Thouvenot, S. Hainzl, D. Marsan, A. Helmstetter, P. Traversa, J. L. Got, L. Jenatton, and R. Guiguet (2011), Changes in effective stress during the 2003-2004 Ubaye seismic swarm, France, *J. Geophys. Res.* **116**, B1, B01309, DOI: 10.1029/2010JB007551.

Enescu, B., and K. Ito (2001), Some premonitory phenomena of 1995 Hyogo-Ken Nanbu (Kobe) earthquake: seismicity, b-value and fractal dimension, *Tectonophysics* **338**, 3-4, 297-314, DOI: 10.1016/S0040-1951(01)00085-3.

Evans, K.F. (2005), Permeability creation and damage due to massive fluid injections into granite at 3.5 km at Soultz: 2. Critical stress and fracture strength, *J. Geophys. Res*. **110**, B4, B04204, DOI: 10.1029/2004JB003169.

Evans, K.F., A. Genter, and J. Sausse (2005a), Permeability creation and damage due to massive fluid injections into granite at 3.5 km at Soultz: 1. Borehole observations, *J. Geophys. Res*. **110**, B4, B04203, DOI: 10.1029/2004JB003168.

Evans, K.F., H. Moriya, H. Niitsuma, R.H. Jones, W.S. Phillips, A. Genter, J. Sausse, R. Jung, and R. Baria (2005b), Microseismicity and permeability enhancement of hydrogeologic structures during massive fluid injections into granite at 3 km depth at the Soultz HDR site, *Geophys. J. Int*. **160**, 1, 389-412, DOI: 10.1111/j.1365-246X.2004.02474.x.

Fischer, T., and A. Guest (2011), Shear and tensile earthquakes caused by fluid injection, *Geophys. Res. Lett.* **38**, 5, L05307, DOI: 10.1029/2010GL 045447.

Fischer, T., S. Hainzl, L. Eisner, S.A. Shapiro, and J. Le Calvez (2008), Microseismic signatures of hydraulic fracture growth in sediment formations: Observations and modeling, *J. Geophys. Res.* **113**, B2, B02307, DOI: 10.1029/2007JB005070.

Gérard, A., A. Genter, T. Kohl, P. Lutz, P. Rose, and F. Rummel (2006), The deep EGS (Enhanced Geothermal System) project at Soultz-sous-Forêts (Alsace, France), *Geothermics* **35**, 5-6, 473-483, DOI: 10.1016/j.geothermics.2006.12.001.

Goto, K., and K. Otsuki (2004), Size and spatial distributions of fault populations: Empirically synthesized evolution laws for the fractal geometries, *Geophys. Res. Lett*. **31**, 5, L05601, DOI: 10.1029/2003GL018868.

Helmstetter, A., G. Ouillon, and D. Sornette (2003), Are aftershocks of large Californian earthquakes diffusing? *J. Geophys. Res.* **108**, B10, 2483, DOI: 10.1029/2003JB002503.

Hill, D.P. (1977), A model for earthquake swarms, *J. Geophys. Res*. **82**, 8, 1347-1352, DOI: 10.1029/JB082i008p01347.

Horálek, J., and T. Fischer (2008), Role of crustal fluids in triggering the West Bohemia/Vogtland earthquake swarms: Just what we know (a review), *Stud. Geophys. Geod.* **52**, 4, 455-478, DOI: 10.1007/s11200-008-0032-0.

Huber, P.J., and E.M. Ronchetti (2011), *Robust Statistics*, 2nd ed., JohnWiley & Sons Inc., New York, 380 pp.

Huc, M., and I.G. Main (2003), Anomalous stress diffusion in earthquake triggering: Correlation length, time dependence, and directionality, *J. Geophys. Res*. **108**, B7, 2324, DOI: 10.1029/2001JB001645.

Kagan, Y.Y. (2007), Earthquake spatial distribution: the correlation dimension, *Geophys. J. Int.* **168**, 3, 1175-1194, DOI: 10.1111/j.1365-246X.2006.03251.x.

Keilis-Borok, V.I., V.G. Kosobokov, and S.A. Mazhkenov (1989), On similarity in the spatial distribution of seismicity, *Vychislitel'naya Seismologiya* **22**, 28-40 (in Russian).

King, G. (1983), The accommodation of large strains in the upper lithosphere of the Earth and other solids by self-similar fault systems: the geometrical origin of b-value, *Pure Appl. Geophys*. **121**, 5-6, 761-815, DOI: 10.1007/BF02590182.

Kosobokov, V.G., and S.A. Mazhkenov (1988), Spatial characteristics of similarity for earthquake sequences: Fractality of seismicity. **In:** *Lecture Notes of the Workshop on Global Geophysical Informatics and Application to Research in Earthquake Prediction and Reduction of Seismic Risk (15 November – 16 December 1988)*, ICTP, Trieste, 1-15.

Kosobokov, V.G., and S.A. Mazhkenov (1994), On similarity in the spatial distribution of seismicity. **In:** D.K. Chowdhury (ed.), *Selected Papers from Volumes 22 and 23 of Vychislitel'naya Seysmologiya*, *Comput. Seismol. Geodyn.*, Vol. 1, AGU, Washington, D.C., 6-15, DOI: 10.1029/CS001p0006.

Lei, X., K. Kusunose, T. Satoh, and O. Nishizawa (2003), The hierarchical rupture process of a fault: an experimental study, *Phys. Earth Planet. In.* **137**, 1-4, 213-228, DOI: 10.1016/S0031-9201(03)00016-5.

Lockner, D.A. (1993), The role of acoustic emission in the study of rock fracture, *Int. J. Rock Mech. Min. Sci. Geomech. Abstr.* **30**, 7, 883-899, DOI: 10.1016/0148-9062(93)90041-B.

Lockner, D.A., and S.A. Stanchits (2002), Undrained poroelastic response of sandstones to deviatoric stress change, *J. Geophys. Res.* **107**, B12, 2353, DOI: 10.1029/2001JB001460.

Lockner, D.A., J.D. Byerlee, V. Kuksenko, A. Ponomarev, and A. Sidorin (1991), Quasi-static fault growth and shear fracture energy in granite, *Nature* **350**, 6313, 39-42, DOI: 10.1038/350039a0.

Lockner, D.A., D.E. Moore, and Z. Reches (1992a), Microcrack interaction leading to shear fracture. **In:** *Proc. 33rd U.S. Rock Mechanics Symposium*, Balkema, Rotterdam, 807-816.

Lockner, D.A., J.D. Byerlee, V. Kuksenko, A. Ponomarev, and A. Sidorin (1992b), Observations of quasistatic fault growth from acoustic emissions. **In:** B. Evans, and T.-F. Wong (eds.), *Fault Mechanics and Transport Properties of Rocks*, Academic Press Inc., New York, 3-31.

Main, I.G., P.G. Meredith, and C. Jones (1989), A reinterpretation of the precursory seismic b-value anomaly from fracture mechanics, *Geophys. J. Int.* **96**, 1, 131-138, DOI: 10.1111/j.1365-246X.1989.tb05255.x.

Marsan, D., C.J. Bean, S. Steacy, and J. McCloskey (2000), Observation of diffusion processes in earthquake populations and implications for the predictability of seismicity systems, *J. Geophys. Res*. **105**, B12, 28081-28094, DOI: 10.1029/2000JB900232.

Mjachkin, V.I., W.F. Brace, G.A. Sobolev, and J.H. Dieterich (1975), Two models for earthquake forerunners, *Pure Appl. Geophys.* **113**, 1, 169-181, DOI: 10.1007/BF01592908.

Mosteller, F., and J.W. Tukey (1977), *Data Analysis and Regression. A Second Course in Statistics*, Addison-Wesley Series in Behavioral Science: Quantitative Methods, Addison-Wesley, Reading, 588 pp.

Nicol, A., J.J. Walsh, J. Watterson, and P.A. Gillespie (1996), Fault size distributions – are they really power-law? *J. Struct. Geol*. **18**, 2-3, 191-197, DOI: 10.1016/S0191-8141(96)80044-7.

Noir, J., E. Jacques, S. Békri, P. M. Adler, P. Tapponnier, and G.C.P. King (1997), Fluid flow triggered migration of events in the 1989 Dobi earthquake sequence of Central Afar, *Geophys. Res. Lett*. **24**, 18, 2335-2338, DOI: 10.1029/97GL02182.

Pandey, A.P., and R.K. Chadha (2003), Surface loading and triggered earthquakes in the Koyna–Warna region, western India, *Phys. Earth Planet. In.* **139**, 3-4, 207-223, DOI: 10.1016/j.pepi.2003.08.003.

Pisarenko, D.V., and V.F. Pisarenko (1995), Statistical estimation of the correlation dimension, *Phys. Lett. A* **197**, 1, 31-39, DOI: 10.1016/0375-9601(94)00923-D.

Pisarenko, V.F. (1989), About recurrence law of earthquakes. **In:** M.A. Sadovsky (ed.), *Discrete Properties of the Geophysical Environment*, Nauka, Moscow, 47-60 (in Russian).

Ponomarev, A.V., A.D. Zavyalov, V.B. Smirnov, and D.A. Lockner (1997), Physical modeling of the formation and evolution of seismically active fault zones, *Tectonophysics* **277**, 1-3, 57-81, DOI: 10.1016/S0040-1951(97)00078-4.

Ponomarev, A., V. Smirnov, A. Patonin, S. Stroganov, and T. Kotlyar (2008), Modeling of transient processes in seismicity: Laboratory experiments (I). **In:** *31th General Assembly of ESC, 7-12 September 2008, Hersonissos, Crete island, Greece*, Abstracts, p. 152.

Reches, Z., and D.A. Lockner (1994), Nucleation and growth of faults in brittle rocks, *J. Geophys. Res*. **99**, B9, 18159-18173, DOI: 10.1029/94JB00115.

Scholz, C.H. (2002), *The Mechanics of Earthquakes and Faulting*, 2nd ed., Cambridge University Press, Cambridge, 471 pp., DOI: 10.1017/CBO9780511818516.

Shapiro, S.A., and C. Dinske (2009), Scaling of seismicity induced by nonlinear fluid-rock interaction, *J. Geophys. Res.* **114**, B9, B09307, DOI: 10.1029/2008JB006145.

Shapiro, S.A., P. Audigane, and J.-J. Royer (1999), Large-scale in situ permeability tensor of rocks from induced microseismicity, *Geophys. J. Int*. **137**, 1, 207-213, DOI: 10.1046/j.1365-246x.1999.00781.x.

Shapiro, S.A., C. Dinske, and J. Kummerow (2007), Probability of a given-magnitude earthquake induced by a fluid injection, *Geophys. Res. Lett.* **34**, 22, L22314, DOI: 10.1029/2007GL031615.

Singh, Ch., P.M. Bhattacharya, and R.K. Chadha (2008), Seismicity in the Koyna–Warna reservoir site in Western India: Fractal and b-value mapping, *Bull. Seismol. Soc. Am*. **98**, 1, 476-482, DOI: 10.1785/0120070165.

Smirnov, V.B. (2003), Estimating the duration of the lithospheric failure cycle from earthquake catalogs, *Izv. – Phys. Solid Earth* **39**, 10, 794-811.

Smirnov, V.B. and A.V. Ponomarev (2004), Regularities in relaxation of the seismic regime according to natural and laboratory data, *Izv. – Phys. Solid Earth* **40**, 10, 807-816.

Smith, W.D. (1981), The b-value as an earthquake precursor, *Nature* **289**, 5794, 136-139, DOI: 10.1038/289136a0.

Sobolev, G.A. (2011), Seismicity dynamics and earthquake predictability, *Nat. Hazards Earth Syst. Sci*. **11**, 445-458, DOI: 10.5194/nhess-11-445-2011.

Sornette, D., and V. Pisarenko (2003), Fractal plate tectonics, *Geophys. Res. Lett*. **30**, 3, 1105, DOI: 10.1029/2002GL015043.

Turcotte, D.L. (1992), *Fractals and Chaos in Geology and Geophysics*, Cambridge University Press, Cambridge, 220 pp.

Vallianatos, F., G. Michas, G. Papadakis, and P. Sammonds (2012), A non-extensive statistical physics view to the spatiotemporal properties of the June 1995, Aigion earthquake (M6.2) aftershock sequence (West Corinth rift, Greece), *Acta Geophys.* **60**, 3, 758-768, DOI: 10.2478/s11600-012-0011-2.

Vlahos, L., H. Isliker, Y. Kominis, and K. Hizanidis (2008), Normal and anomalous diffusion: A Tutorial. **In:** T. Bountis (ed.), *Order and Chaos*, Vol. 10, Patras University Press, Patras.

Watterson, J., J.J. Walsh, P.A. Gillespie, and S. Easton (1996), Scaling systematics of fault sizes on a large-scale range fault map, *J. Struct. Geol*. **18**, 2-3, 199-214, DOI: 10.1016/S0191-8141(96)80045-9.

Wiemer, S., and M. Wyss (2000), Minimum magnitude of completeness in earthquake catalogs: examples from Alaska, the western United States, and Japan, *Bull. Seismol. Soc. Am*. **90**, 4, 859-869, DOI: 10.1785/0119990114.

Yielding, G., T. Needham, and H. Jones (1996), Sampling of fault populations using sub-subsurface data: a review, *J. Struct. Geol*. **18**, 2-3, 135-146, DOI: 10.1016/S0191-8141(96)80039-3.

Zavyalov, A.D. (2002), Testing the MEE prediction algorithm in various seismically active regions in the 1985-2000 period: Results and analysis, *Izv. – Phys. Solid Earth* **38**, 4, 262-275.

Zhang, G., and Z. Fu (1981), Some features of medium- and short-term anomalies before great earthquakes. **In:** D.W. Simpson and P.G. Richards (eds.), *Earthquake Prediction. An International Review*, Maurice Ewing Series, Vol. 4, AGU, Washington, D.C., 497-509, DOI: 10.1029/ME004p0497.

Zhurkov, S.N. (1965), Kinetic concept of the strength of solids, *Int. J. Fract. Mech*. **1**, 4, 311-323.

Zhurkov, S.N., V.S. Kuksenko, V.A. Petrov, V.N. Savlyev, and U. Sultanov (1977), On the problem of prediction of rock fracture, *Izv. –Phys. Solid Earth* **13**, 6, 374-379.

Received 27 November 2012
Received in revised form 30 March 2013
Accepted 10 April 2013